Decomposition and adaptive filtering using binomial filter bank for ground-roll attenuation

Cristian Ariza*, CPGG/IGEO/UFBA, Milton J. Porsani, CPGG/IGEO/UFBA & INCT-GP/CNPq/Brazil

This paper was prepared for presentation during the 15th International Congress of the Brazilian Geophysical Society, held in Rio de Janeiro, Brazil, 31 July to 3 August 2017.

Abstract

The ground-roll is a type of noise associated with land seismic data. It strongly harms the signal-to-noise ratio, and interferes in various stages of the seismic data processing, affecting the final quality of the obtained seismic images. In this paper we propose a method of adaptive filters using binomial filters built from the convolution of pairs of dipoles $(1,c)$ e $(c,-1)$ for the attenuation of the ground-roll, where c is the first coefficient prediction error calculated by Burg algorithm. It allows for the decomposition of signals in frequency bands from the lowest to the highest adapting to frequency content of the data. Its implementation and use in the processing of seismic data is relatively simple and computationally efficient.

Introduction

One of the most significant challenges in processing of seismic data is to filter different types of noises. Ground roll is one of the main types of coherent noise in land seismic data. It has the significant characteristics of relatively low velocity, low frequency, high amplitude and strong energy (Sheriff, 2002). Because of its dispersive nature and low velocity, ground-roll masks the shallow reflections at near offsets and deep reflections at far offsets (Saatcilar and Canitez, 1988; McMechan and Sun, 1991; Saatcilar and Canitez, 1994; Henley, 2003) and also distorts reflection events by interfering with them.

Ground-roll (GR), is one of the main coherent noises in petroleum seismic exploration, many methods have been introduced to attenuate this type of noise. Although the right choice of attenuation techniques is a matter of trial and error (Sheriff and Geldart, 1995). The conventional methods can be divided into two groups. The first one can be summarized to filter method which is based on suppression of undesired parts of recorded data in the spectral domain, including high-pass and band-pass filtering, $f-k$ filtering (Embree et al., 1963; Treitel et al., 1967; Yilmaz, 2001) and the adaptive ground-roll attenuation method (Wang et al., 2012; Hosseini et al., 2015). These methods have their limitations. High-pass and band-pass filter may eliminate the low frequency component of effective waves since the frequency bands of ground-roll noise and reflections are often overlapped (Sirgue, 2006). The conventional $f-k$ filter would cause serious distortion of effective waves when the energy of ground-roll noise is much stronger than that of reflections (McMechan and Sun, 1991; Liu, 1999; Tokeshi et al., 2006). The other one is wave field separation method based on ground-roll noise extraction and arithmetical subtraction of it from the raw shot gather in the tâx domain, including Wienerâ Levinson algorithm (Karslı and Bayrak, 2004), Karhunen-Loève (K-L) transform (Gómez Londoño et al., 2005), wavelet transform (Deighan and Watts, 1997a) and Radon transform (Russell et al., 1990a,b).

There are different methods of decomposing a seismic signal used for suppressing the ground-roll: Decomposition Empirical Mode (DME), developed by Huang et al. (1998) and used by Ferreira et al. (2013); singular value decomposition, SVD used by Porsani et al. (2010), Wavelet decomposition used by Deighan and Watts (1997b), decomposition by filtering frequency bands with binomial operators justified by Akansu and Haddad (2001) and Vetterli and Herley (1992) used by Ariza and Porsani (2015) for attenuation ground-roll.

Filtering with binomial operators (Haddad (1971), Akansu and Haddad (2001), Vetterli and Herley (1992)), enable decomposition and perfect reconstruction of the signal through the linear combination of its components. The decomposition of a signal is made into frequency bands by means of a matrix operators $\widetilde{\mathbf{X}}$, which is obtained by weighting each of the columns of the matrix $\mathbf{X}_n^j$ (obtained through the dipoles $(1,1)$ and $(1,-1)$) with k coefficient of a given column a matrix $\mathbf{X}^{-1}$, or $\mathbf{X^{-1}}_k^a$. This procedure allows for the original signal shifted to the position $\widetilde{S}_n = S_n * \delta_{n-a}$. To recover the signal in the initial position just delay it for a samples.

It can be shown that the construction of the matrix $\mathbf{X}$, through the dipoles $(1,1)$ and $(1,\ -1)$, is just a special case of a general breakdown binomial with dipoles (α,β) and $(\beta,\ -\alpha)$ where α and β can be real or complex (in this work we will only consider the case real), where the values of α and β beta can be arbitrarily chosen or may be obtained by the features given itself, creating infinite possibilities of decomposition. This work are used dipoles adaptively with $(1,c)$ and $(c,-1)$ for filtering the ground-roll, where c is the first prediction error coefficient calculated with the burg algorithm.

Theory

Following is presented a form of general binomial decomposition with dipoles (α,β) e $(\beta,-\alpha)$, where α and β can be real or complex (in this text we will only consider the real case). The dipoles $(1,1)$ e $(1,-1)$ are a special case of this representation general (Boyd et al., 2001; Severo and Schillo, 2009; Severo, 2008).

In the case of a binary decomposition of order 1 ($N=1$), the operators matrix $\mathbf{X}$ is written as follows:

$$\mathbf{X} = \begin{bmatrix} \alpha & \beta \\ \beta & -\alpha \end{bmatrix} = \begin{bmatrix} \mathbf{y}_0^T \\ \mathbf{y}_1^T \end{bmatrix} = \begin{bmatrix} \mathbf{x}_0 & \mathbf{x}_1 \end{bmatrix} \qquad (1)$$

You can verify that $\mathbf{X}^2 = \lambda \mathbf{I}$. For the case where $N = 1$, $\lambda = \alpha^2 + \beta^2$, so the matrix $\mathbf{X}^{-1}$ is:

$$\mathbf{X}^{-1} = \frac{1}{\alpha^2+\beta^2}\begin{bmatrix} \alpha & \beta \\ \beta & -\alpha \end{bmatrix} = \begin{bmatrix} \frac{\alpha}{\alpha^2+\beta^2} & \frac{\beta}{\alpha^2+\beta^2} \\ \frac{\beta}{\alpha^2+\beta^2} & \frac{-\alpha}{\alpha^2+\beta^2} \end{bmatrix} \quad (2)$$

The operator matrix $\widetilde{\mathbf{X}}$ is obtained, for example, selecting the first column of $\mathbf{X}^{-1}$ ($a = 0$). This results in

$$\widetilde{\mathbf{X}}^0 = \begin{bmatrix} \frac{\alpha^2}{\alpha^2+\beta^2} & \frac{\beta^2}{\alpha^2+\beta^2} \\ \frac{\alpha\beta}{\alpha^2+\beta^2} & \frac{-\alpha\beta}{\alpha^2+\beta^2} \end{bmatrix} \quad (3)$$

It should be noted that if the columns of the matrix $\widetilde{\mathbf{X}}$ are added together, the result is $(1,0)^T$.

Applying binary decomposition of order 1 ($N = 1$) to a discrete signal $\{S_n\} = \{s_0,\ldots,s_{M-1}\}$ is equivalent to performing the convolution of the original signal with each of the columns of the operator matrix $\widetilde{\mathbf{X}}^0$. The signal recovery is obtained by a simple addition of signal components.

$$\begin{aligned} \{R_n\} &= \{S_n\} * \{\widetilde{X}_0^0\} + \{S_n\} * \{\widetilde{X}_1^0\} \\ &= \{S_n\} * \{\widetilde{X}_0^0 + \widetilde{X}_1^0\} \\ &= \{S_n\} * (1,0)^T = \{S_n\} * \{\delta_n\} \\ &= \{S_n\} \end{aligned} \quad (4)$$

The operators matrix $\mathbf{X}$ for any order N (where $\mathbf{X}$ have $N+1$ columns) is calculated as follows:

$$X_n^r = (\alpha,\beta)^{*(N-r)} * (\beta,-\alpha)^{*r} \quad (5)$$

for $0 \le r \le N$. Remember that

$$x^{*n} = \underbrace{x * x * x * \cdots * x * x}_{n} \quad (6)$$

denotes n-times convolution, where $x^{*0} = \delta_0$, $x^{*1} = x$ and δ_0 is the Kronecker delta.

The matrix generated as shown above keeps the property of orthogonality between rows and columns, i.e., $\mathbf{y}_i^T \mathbf{x}_j = 0$ for $i \neq j$ and $\mathbf{y}_i^T \mathbf{x}_j = \lambda^N$ for $i = j$. That is

$$\mathbf{X}^2 = \lambda^N \mathbf{I} \quad (7)$$

where

$$\lambda = \alpha^2 + \beta^2 \quad (8)$$

calculating the inverse matrix as

$$\mathbf{X}^{-1} = \frac{\mathbf{X}}{\lambda^N} \quad (9)$$

The property $\mathbf{X}^2 = \lambda^N \mathbf{I}$ is particularly important in signal decomposition and filtering. We note that, despite of a scale factor, λ^N, $\mathbf{X}$ matrix is its own inverse, since the product it generates by itself is a diagonal matrix. This property provides $N+1$ possibilities to decompose the original signal, each related to a particular column of the matrix $\widetilde{\mathbf{X}}^a$ ($a = 0,1,\ldots,N$). The signal can be decomposed or rebuilt as a linear combination of components, obtained by convolution of the original signal with the columns of the matrix $\widetilde{\mathbf{X}}^a$. Each component, $\{\widetilde{S}_n^r\} = \{\widetilde{X}_n^r\} * \{S_n\}$, will have a different frequency content depending on the values α and β selected.

The values of α and β can be arbitrary or be calculated using the characteristics of the data $\{S_n\} = \{s_0,\ldots,s_{M-1}\}$ (which is adaptive). Consequently, the method is versatile and has many ways to achieve the decomposition of the signal $\{S_n\}$ used for signal analysis or filtering.

Result

In order to get local information from the data, the recursive Burg algorithm was used to obtain the first coefficient of prediction error for a specified window's length (Burg, 1967). It is possible to generate dipoles $(1,c)$ e $(c,-1)$, where c is the first prediction error coefficient, for a given window. Taking into account the minimum phase property of the linear unit error prediction filters when they are calculated using the least squares method (Appendix A of Chu (2004)), the first coefficient is always negative less than one, then the first dipole $(1,c)$ is a differentiation operator allowing the capture of high frequency information (depending on the window width) and the second dipole $(c,-1)$ (both negative) would be an operator of integration which allows capturing low-frequency information.

We use a 96-channel common-shot-point gather (Figure 6A) acquired in the North-west Brazil (Tacutu Basin) to demonstrate the feasibility and applicability of the proposed method. The geophone interval is 50 m. The length of the record is 4000 ms with a 4 ms sample interval.

There were tested different window sizes (from 20 to 2000 ms), achieving the best contrast between areas with and without GR with a 200 ms window. In figure 1 the coefficient values are shown and the contrast between areas with and without GR are very clear (Compared with Figure 6A).

For the desing of the map of Figure 1, the following procedure was followed for each trace:

- The coefficient map begins with a value of 0.0.
- The value of the first coefficient error for the window's length is calculated using the Burg Algorithm.
- The coefficient value is added to all the positions of the window's length in the coefficient map.
- The window is then moved one sample, and the previous two steps are repeated until the end of the trace.

At the end, an average is calculated as a function of the number of values added at each position of the coefficient map. This procedure is presented in the algorithm 1.

The algorithms used to trace decomposition are shown bellow (Algorithm 2 and Algorithm 3).

Decomposition and reconstruction of signal

To test the decomposition and perfect reconstruction of the signal it was used a level of decomposition $N = 7$

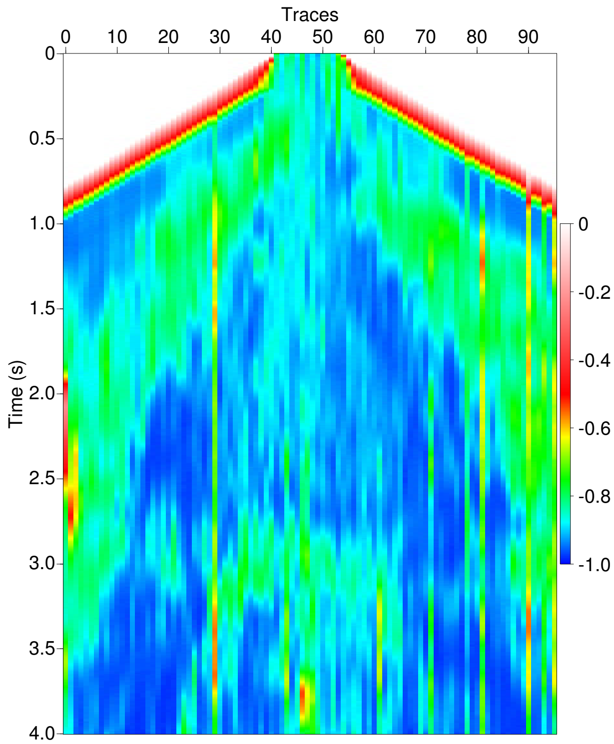

Figure 1: Representation of the first prediction error coefficient for Burg algorithms

weighted by the first column of the inverse matrix ($a = 0$), so the signal is decomposed into 8 shot gather with different frequency content from highest to lowest. In the Spectral analysis (average spectra of all traces, Figure 2) of each sub-image it is evident the effect on the amplitude distribution. Generally almost all sub-images have lower amplitude than the original. In the four shot gather shown in Figure 3 (only four of the eight total sub-images are depicted for cleaner presentation), it can be seen that each shot gather has different frequency content. Air wave (or sound wave) noise exists, which can be identified in $\widetilde{S}_1$ with an apparent velocity of about 340 m/s (Figure 3A). It is evident that air wave is a type of non-dispersive coherent noise, as same as body wave. As seen in sub-image $\widetilde{S}_7$, reflections are heavily contaminated by largely dispersed ground-roll noise (Figure 3D). Remember that our signal has more information between 0 and 50 Hz of the amplitude spectrum. The differences between the first sub-images corresponding to higher frequencies are minimal. The sum of these eight shot gathers reconstruct the original shot gather with a very small error (Figure 4).

Ground-roll attenuation

The weak reflections are invisible due to the interference of the strong ground-roll noise (Figure 6A). Furthermore, the waveforms of the shot gather are even truncated at some places due to this high-amplitude ground-roll noise. We can see that there is mostly the energy of ground-roll noise within the frequency band from 1 to 10 Hz. The energy of ground-roll noise and effective waves is also obvious within the frequency band from 10 to 20 Hz. In the

Algorithm 1 Prediction error coefficients map

Require: $S(ns)$: Entry trace (number of samples); Lw: Window's length;
Initialize $Mp(ns) = 0.0$; $x(Lw) = 0.0$; $y(Lw) = 0.0$; $z(ns) = 0.0$;
for $i = 1, ns - Lw + 1$ **do**
  $x(1 : Lw) \leftarrow S(i : i + Lw - 1)$;
  Compute c for $x(Lw)$; Burg algorithms
  $y(1 : Lw) \leftarrow c$;
  $Mp(i : i + Lw - 1) \leftarrow Mp(i : i + Lw - 1) + y(Lw)$;
  $z(i : i + Lw - 1) \leftarrow z(i : i + Lw - 1) + 1$;
end for
$Mp(j) \leftarrow Mp(j)/z(j)$; $j = 1, \ldots, ns$
return Map error $Mp(ns)$

Algorithm 2 Trace decomposition

Require: $S(ns)$: Input trace (number of samples); Lw: long window; N: level of decomposition;
initial $\mathbf{DS}(ns, N + 1) = 0.0$; $x(Lw) = 0.0$; $\mathbf{Y}(Lw, N + 1) = 0.0$; $z(ns) = 0.0$
for $i = 1, ns - Lw + 1$ **do**
  $x \leftarrow S(i : i + Lw - 1)$;
  $\mathbf{Y} \leftarrow$ Compute window decomposition of x ;
  $\mathbf{DS}(i : i + Lw - 1, :) \leftarrow \mathbf{DS}(i : i + Lw - 1, :) + \mathbf{Y}$;
  $z(i : i + Lw - 1) \leftarrow z(i : i + Lw - 1) + 1$;
end for
$\mathbf{DS} \leftarrow DS(j, :) \leftarrow DS(j, :)/z(j)$; $j = 1, \ldots, ns$
return Decomposed trace $\mathbf{DS}(ns, N + 1)$

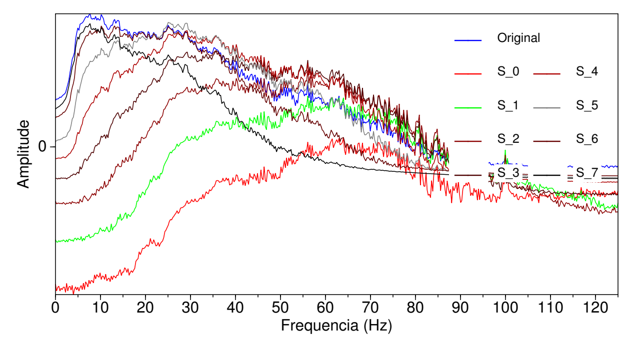

Figure 2: Spectral analysis of the decomposition shot gather with dipoles $(1, c)$ e $(c, -1)$ for $N = 7$.

frequency band above 20 Hz, there is mostly the energy of the effective waves (Figure 2 and Figure 5).

By using the proposed decomposition method, the ground-roll noise is successfully separated out from the shot signal (Figure 3D). Observing the amplitude spectra generated by decomposition (Figure 2), the sub-images $\widetilde{S}_6$ and $\widetilde{S}_7$ are those that have greater low frequency content. Hence, a good option to mitigate the GR is to reconstruct the signal by adding the sub-images $\widetilde{S}_0$ to $\widetilde{S}_5$ (DB1c) or, likewise, subtracting $\widetilde{S}_6$ and $\widetilde{S}_7$ from original shot.

To validate the results of this method there were applied two chosen methods frequently used: trapezoidal frequency bandpass filter ($f_1 = 10$, $f_2 = 20$, $f_3 = 60$, and $f_4 = 70Hz$ are the corner frequencies) and $f - k$ filtering.

Spectral analysis (Figure 5) shows the results of these

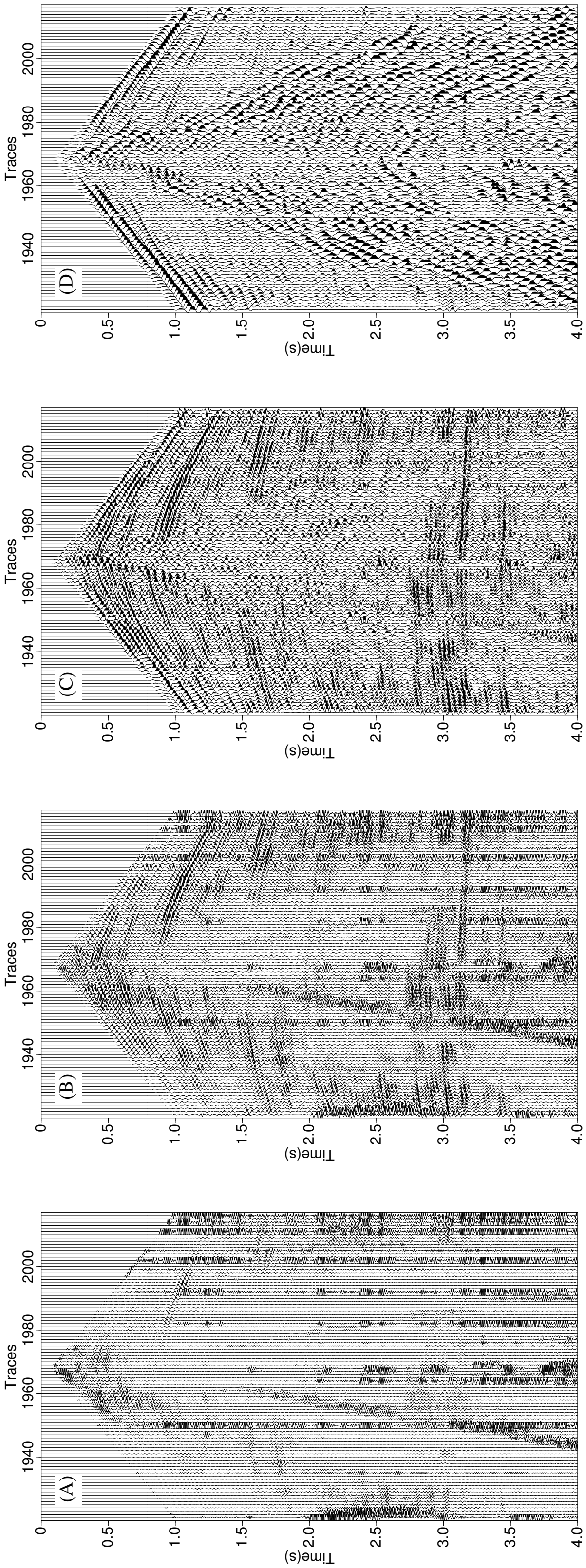

Figure 3: Adaptive Binomial decomposition $N = 7$. Only four of the eight sub-images are shown: (A) $\widetilde{S}_1$, (B) $\widetilde{S}_3$, (C) $\widetilde{S}_5$ and (D) $\widetilde{S}_7$.

Algorithm 3 Window decomposition

Require: $x(Lw)$: Input (number of samples); N: level of decomposition; $a = 0$: Weighting column.

initial $\mathbf{X}(N+1,N+1) = 0$; $\widetilde{\mathbf{X}}(N+1,N+1) = 0$; $\mathbf{Y}(Lw+N,N+1) = 0$;
if $\sum|x| > 0$ **then**
  Compute c with Burg algorithm
  $\mathbf{X} \leftarrow X_n^r = (1,c)^{*(N-r)} * (c,-1)^{*r} \qquad r = 0,1,\ldots,N$
  $\lambda \leftarrow \alpha^2 + \beta^2$; $\alpha = 1$; $\beta = c$
  $\mathbf{X}^{-1} \leftarrow \mathbf{X}/\lambda^N$
  $\widetilde{\mathbf{X}} \leftarrow \widetilde{X}(:,j) \leftarrow X(:,j) \cdot X^{-1}(j,a); \qquad j = 0,1,\ldots,N$
  $\mathbf{Y} \leftarrow Y(:,j) \leftarrow x * \widetilde{X}(:,j); \qquad j = 0,1,\ldots,N$
else
  $\mathbf{Y} = 0.0$
end if
return Decomposed window $\mathbf{Y}(Lw,N+1)$

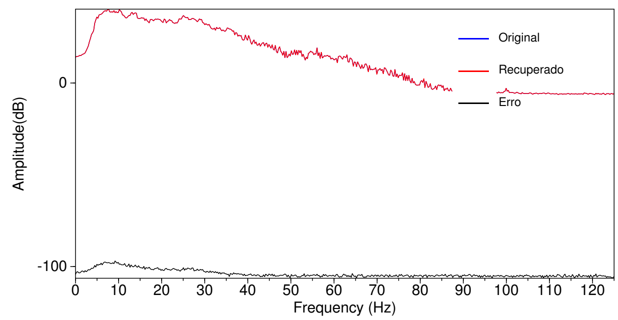

Figure 4: Spectral analysis of the shot gather and perfect reconstruction results . The red line, the blue line, and the black line denote spectra of original data, perfect reconstruction and error, respectively. (Red and blue lines are coincident). The amplitude is in logarithmic scale.

two compared methods. Band-pass filter eliminates the low frequency component of the signal and since the frequency bands of ground-roll noise and reflections are overlapped, the effective waves energy has been seriously damaged. The $f-k$ filter still contains relatively (compared to effective waves, 30 Hz) strong ground-roll noise in the frequency band from 0 to 20 Hz, whereas the proposed method (DB1c) has remove most of the ground-roll noise conserving the effective waves energy and some fraction of low frequency component.

All three methods provide ways to extract ground-roll, but band-pass filter has significant decrease amplitude drawback. $f-k$ filtering causes serious distortion of effective waves because the energy of ground-roll noise is much stronger than that of reflections. We can conclude that the results of the adaptive ground roll attenuation method is the best among these (Figure 6).

Conclusions

Taking into account the properties of the binomial operator it is possible to perform signal decomposition and subsequent recovery at any level using binomials $(1,c)$ and $(c,-1)$. This method's filters showed superior results in ground-roll attenuation compared with the filtering in the frequency domain (1D), highlighting the conservation of a fraction of the low frequencies necessary for further

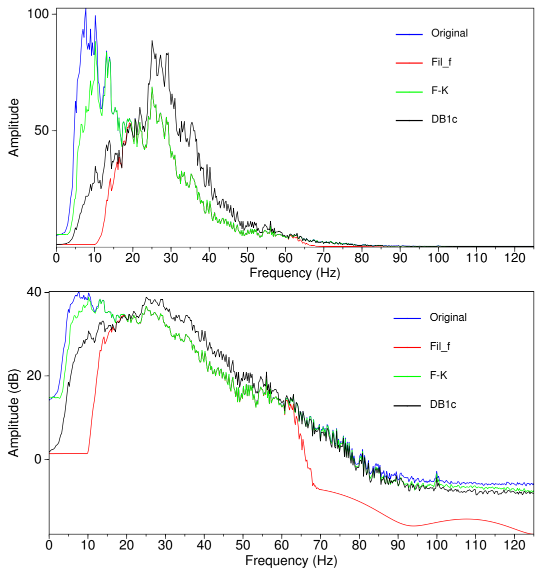

Figure 5: Spectral analysis of the shot gather and results of all three filtering methods in 6. The red line, the blue line, the green line, and the black line denote spectra of original data, results after band-pass, $f-k$, and the proposed method's (DB1c) filtering, respectively. The amplitude is in linear scale (above) and logarithmic scale (below).

processing of the signal.

As general characteristics of binomial filters one can mention the following:

- The implementation of the bank of binomial filters at any level allows perfect reconstruction of seismograms;
- Any additional processing may be performed in any of the sub-images, which makes the method very versatile;
- The generation of adaptive binomial operator (filter) only involves dipoles convolution and their use in filtering of seismic data is considerably simple and computationally efficient;
- The signal decomposition is performed trace by trace which allows parallelization of the processing of very large data volumes;
- The results of the *ground-roll* filtering illustrate the applicability of binomial method in seismic data processing;
- The algorithm is robust, easy to implement, computationally efficient and requires less parameter setting by the user.

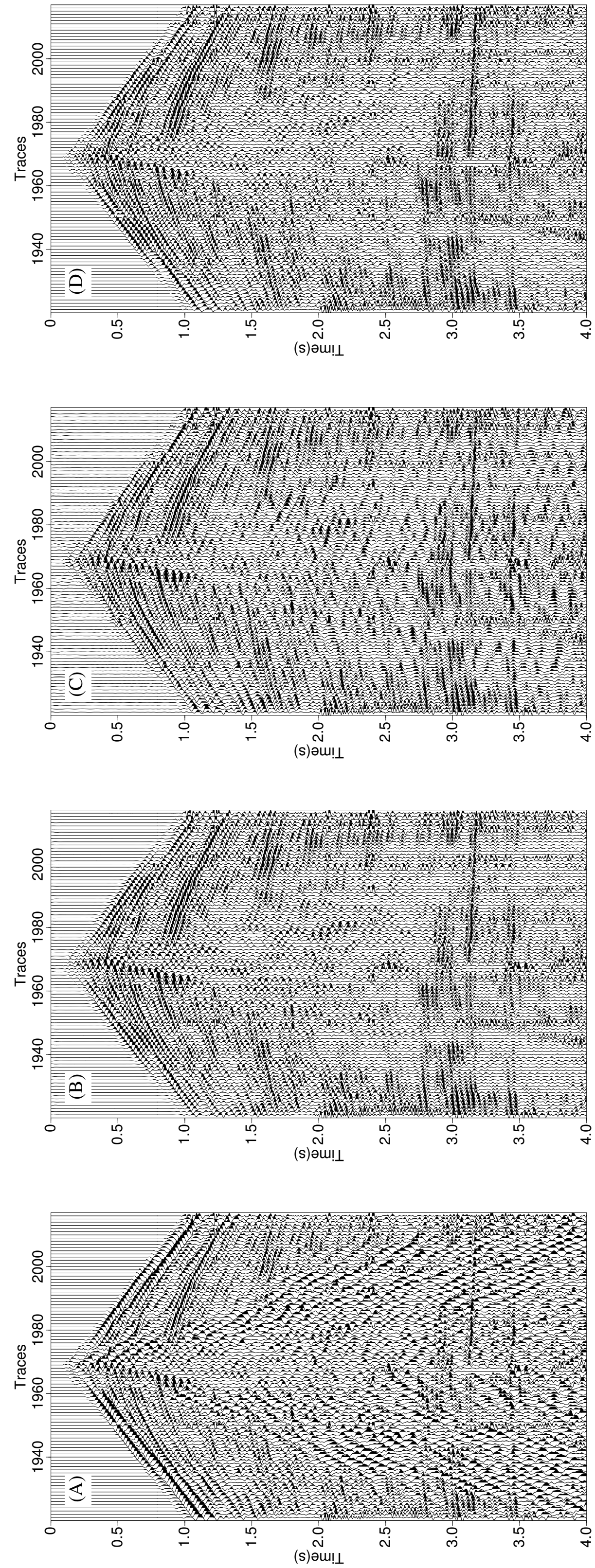

Figure 6: (A), (B), (C), and (D) are the original shot, results after band-pass, $f-k$, and the proposed method's (DB1c) filtering, respectively.

Acknowledgements

The authors wish to express their gratitude to the Fundação de Amparo à Pesquisa do Estado da Bahia (FAPESB), INCT-GP, (CNPq), FINEP, PETROBRAS, Brazil, for financial support.

References

Akansu, A. N. and R. A. Haddad, 2001, Multiresolution signal decomposition: Transforms, subbands, and wavelets, 2nd ed. Series in Telecommunications: Academic Press.

Ariza, C. and M. J. Porsani, 2015, Atenuação do ground-roll utilizando filtros binomiais: 14th International Congress of the Brazilian Geophysical Society & EXPOGEF, Rio de Janeiro, Brazil, 3-6 August 2015, 1345–1350.

Boyd, G., C. A. Micchelli, G. Strang, and D.-X. Zhou, 2001, Binomial matrices: Advances in Computational Mathematics, **14**, 379–391.

Burg, J. P., 1967, Maximum entropy spectral analysis.: 37th Annual International Meeting., 34–41.

Chu, W. C., 2004, Speech coding algorithms: foundation and evolution of standardized coders: John Wiley & Sons.

Deighan, A. J. and D. R. Watts, 1997a, Ground-roll suppression using the wavelet transform: Geophysics, **62**, 1896–1903.

——, 1997b, Ground-roll suppression using the wavelet transform: Geophysics, **62**, 1896–1903.

Embree, P., J. P. Burg, and M. M. Backus, 1963, Wide-band velocity filtering-the pie-slice process: Geophysics, **28**, 948–974.

Ferreira, L. E. S., M. J. Porsani, M. G. da Silva, and G. L. Vasconcelos, 2013, Application of the empirical mode decomposition method to gound-roll noise attenuation in sismic data: Revista Brasileira de Geofísica, **31**, 619–630.

Gómez Londoño, E., L. Castillo López, and K. Thaís de Souza, 2005, Using the karhunen-loève transform to suppress ground roll in seismic data: Earth Sciences Research Journal, **9**, 139–147.

Haddad, R. A., 1971, A class of orthogonal nonrecursive binomial filters: Audio and Electroacoustics, IEEE Transactions on, **19**, 296–304.

Henley, D. C., 2003, Coherent noise attenuation in the radial trace domain: Geophysics, **68**, 1408–1416.

Hosseini, S. A., A. Javaherian, H. Hassani, S. Torabi, and M. Sadri, 2015, Adaptive attenuation of aliased ground roll using the shearlet transform: Journal of Applied Geophysics, **112**, 190–205.

Huang, N. E., Z. Shen, S. R. Long, M. C. Wu, H. H. Shih, Q. Zheng, N.-C. Yen, C. C. Tung, and H. H. Liu, 1998, The empirical mode decomposition and the hilbert spectrum for nonlinear and non-stationary time series analysis: The Royal Society, **454**, 903–995.

Karslı, H. and Y. Bayrak, 2004, Using the wiener–levinson algorithm to suppress ground-roll: Journal of Applied Geophysics, **55**, 187–197.

Liu, X., 1999, Ground roll supression using the karhunen-loeve transform: Geophysics, **64**, 564–566.

McMechan, G. and R. Sun, 1991, Depth filtering of first breaks and ground roll: Geophysics, **56**, 390–396.

Porsani, M. J., M. G. Silva, P. E. M. Melo, and B. Ursin, 2010, Svd filtering applied to ground-roll attenuation: Journal of Geophysics and Engineering.

Russell, B., D. Hampson, and J. Chun, 1990a, Noise elimination and the radon transform, part 1: The Leading Edge, **9**, 18–23.

——, 1990b, Noise elimination and the radon transform, part 2: The Leading Edge, **9**, 31–37.

Saatcilar, R. and N. Canitez, 1988, A method of ground-roll elimination: Geophysics, **53**, 894–902.

——, 1994, The lattice filter in ground-roll suppression: Geophysics, **59**, 623–631.

Severo, N. C., 2008, Matrices with convolutions of binomial functions and krawtchouk matrices: Linear Algebra and its Applications, **429**, 50–56.

Severo, N. C. and P. J. Schillo, 2009, Matrices whith convolutions of binomial functions, their determinants, and some examples: Journal of Algebra, Number Theory: Advances and Applications, **2**, 51–57.

Sheriff, R. E., 2002, Encyclopedic dictionary of applied geophysics.

Sheriff, R. E. and L. P. Geldart, 1995, Exploration seismologycambridge university press.

Sirgue, L., 2006, The importance of low frequency and large offset in waveform inversion: Presented at the 68th EAGE Conference and Exhibition incorporating SPE EUROPEC 2006.

Tokeshi, J. C., M. B. Karkee, and Y. Sugimura, 2006, Reliability of rayleigh wave dispersion curve obtained from f–k spectral analysis of microtremor array measurement: Soil Dynamics and Earthquake Engineering, **26**, 163–174.

Treitel, S., J. L. Shanks, and C. W. Frasier, 1967, Some aspects of fan filtering: Geophysics, **32**, 789–800.

Vetterli, M. and C. Herley, 1992, Wevelet and filter banks: theory and desing: IEEE Transaction on sinal processing, 2207–2232.

Wang, W., J. Gao, W. Chen, and J. Xu, 2012, Data adaptive ground-roll attenuation via sparsity promotion: Journal of Applied Geophysics, **83**, 19–28.

Yilmaz, O., 2001, Seismic data analysis: Society of exploration.